

INFLUENCE OF THERMOCOUPLE THERMAL INERTIA IN IMPINGEMENT HEAT TRANSFER EXPERIMENTS USING TRANSIENT TECHNIQUES

Alexandros Terzis¹, Jens von Wolfersdorf², Guillaume Wagner³, Bernhard Weigand² and Peter Ott¹

¹Group of Thermal Turbomachinery (GTT), École Polytechnique Fédérale de Lausanne (EPFL)
CH-1015, Lausanne, Switzerland

²Institute of Aerospace Thermodynamics (ITLR), Universität Stuttgart
Pfaffenwaldring 31, D-70569, Stuttgart, Germany

³Alstom, Baden, Switzerland

ABSTRACT

A typical transient heat transfer experiment for an impingement cooling configuration requires usually a temperature step in the flow. A moving isotherm of the liquid crystal surface coating is then monitored using a video camera. However, for small impingement configurations, when only a small number of holes is used, the massflow rates are relatively low, leading to very small plenum velocities. Therefore, a step change in the power settings does not cause a temperature step in the mainstream flow. Many researchers approximated the real hot gas temperature evolution by a number of ideal temperature steps (Duhamel's superposition principle). However, thermocouple acquisition measurements are influenced by the size of the thermocouple due to thermal inertia and therefore direct evaluation of the heat transfer coefficient with these data may be in error. This paper suggests that the hot gas temperature which drives the transient experiment and is measured in the plenum can be corrected according to the time constant of the thermocouples. Several experiments were carried out in order to evaluate the time response of fine thermocouples with exposed junction. For the impingement configuration, a single row of five inline impingement holes is used at in a narrow passage configuration over a range of Reynolds numbers (15000-55000). The liquid crystal signal is evaluated with three different hot gas temperature approaches: (1) *Perfect temperature step*, (2) *Duhamel's principle in the acquired temperature data* and (3) *Correction of hot gas temperature for thermal inertia prior to Duhamel's principle*. The experimental data are analyzed by means of various post-processing procedures and aim to clarify and quantify the effect of thermocouple thermal inertia on the final results.

INTRODUCTION

Turbine blade impingement cooling finds great applicability in modern gas turbine engines providing enhanced heat transfer capabilities compared to traditional convective cooling passages while the continuously injected coolant flow ensures very high heat fluxes in the stagnation region of the jets. A detailed review for multi-jet impingement configurations can be found e.g. in the review paper of Weigand and Spring (2011) [1].

One of the most famous measurement techniques which is used to evaluate the heat transfer characteristics of impingement cooling systems is the transient liquid crystal technique which finds great applicability in turbomachinery applications over the last 20 years. Detailed reviews of the applied method and its applications can be found e.g. Baughn (1995) [2], Ireland (1999) [3], Ireland and Jones (2000) [4] and Poser and von Wolfersdorf (2011) [5]. The main advantages of this technique are the direct local temperature measurement over the test surface with high resolution and the non-intrusive measurement. With other words, this technique uses the full surface temperature history derived from the color of the liquid crystals in order to obtain full surface heat transfer coefficient distributions on the examined surfaces.

Van Treuren *et al.* (1994) [6] developed the first test rig capable for a transient liquid crystal experiment measuring both the local adiabatic wall temperature and the local heat transfer coefficient under an array of impinging jets. The idea in this work was to create a sudden temperature step in the flow using a heat exchanger. The temperature step was achieved by switching properly valves and bypass flow so that hot air from an introductory plenum chamber was then introduced inside the impingement array forcing the color change of the liquid crystals. A similar test rig was used by Huang and El-Genk (1994) [7]. They supplied

¹ Contact details: Alexandros Terzis

Group of Thermal Turbomachinery (GTT), ME A2 475, EPFL SCI-STI-PO
Swiss Federal Institute of Technology, CH1015, Lausanne, Switzerland
Tel: +41 (0) 21 693 3539 / E-mail: alexandros.terzis@epfl.ch

compressed air in an electric heater and a three-way ball diverted valve was used in order to isolate the main flow from the plenum chamber of the test rig. Once the conditions were stabilized, switching off the valve allowed hot gas to enter the plenum chamber and initiated the transient experiment. However, the main disadvantage of fast acting valves is the complexity of the design and that the mainstream temperature rise cannot be represented as a real step. Other approaches include rapidly inserting a model into a wind tunnel of a constant mainstream temperature which is higher than the initial model temperature, as for example in the studies of Falcoz *et al.* (2006) [8] and Wagner *et al.* (2007) [9]. However, the performance of any mechanical injection system is highly dependent on the size of the test rig and hence the inertia forces of the test model. Obviously, the large scale impingement test models which are usually required for higher resolution and increased Reynolds numbers cannot be assumed suitable for pneumatic insertion mechanisms.

The mechanical complexities of fast acting valves or model positioning activators can be avoided using the concept of a heater mesh, originally developed by Gillespie *et al.* (1995) [10]. The heater mesh is used in order to increase the temperature of the mainstream flow taking advantage of *Joule Heating*. Additionally, the temperature step achieved with a heater grid configuration is relatively quick and thus ideal for a transient heat transfer experiment (Esposito *et al.* (2009) [11]). However, in many experiments, and especially for small impingement configurations where the number of holes is low, the massflow rates are relatively small leading to very low plenum velocities ($<1m/s$). As a result, a step change in the power settings does not cause a step change in the flow temperature. Many researchers used Duhamel's superposition principle assuming a series of step changes in the mainstream temperature, although the accuracy of this method requires a relatively small time step and thus high acquisition rate, as shown by Kwak (2008) [12]. An additional concern at this velocity level is that the thermocouple measurements are influenced by their response time. In such cases, it is quite difficult to determine the hot gas temperature which drives the transient experiment and a correction based on their response time should be applied in order to increase the accuracy of the results. Most of the attempts made to measure experimentally response time of thermocouples involve submersion of the thermocouple inside a liquid bath and the time required to reach 63.2% of the steady state bath temperature was considered as the response time for the given thermocouple (Wormser (1960) [13], Murdock *et al.* (1963) [14]). However, these methods appear to be inappropriate when the thermocouples are subjected to a gas stream. On the other hand, attempts to measure the response time of fine thermocouples in air are limited in the open literature. Farahmand and Kaufman (2001) [15] carried out experiments in order to evaluate thermocouple response time applying velocities above 2m/s and small temperature changes ($10-15^{\circ}C$) which are not consistent with the requirements of many transient heat transfer experiments in impingement cooling applications when the jets are fed from the same plenum chamber.

In this study, the time constant of various K-type thermocouples with exposed junction was experimentally evaluated. Thermocouple thermal inertia characteristics are discussed in details as well as their effect on the calculation of the heat transfer coefficient. For the evaluation of the heat transfer distributions three different scenarios have been considered: (1) Perfect temperature step in the flow (2) Series of step changes (Duhamel's superposition principle) on the acquired thermocouple measurements (3) Series of step changes on the corrected hot gas temperature considering thermocouple thermal inertia characteristics. The results indicate that the calculated heat transfer level is highly affected by the evolution of the hot gas temperature.

NOMENCLATURE

D	=	impingement hole diameter (m)
d	=	thermocouple wire diameter (m)
c	=	specific heat ($J/(kgK)$)
h	=	heat transfer coefficient ($W/(m^2K)$)
k	=	thermal conductivity ($W/(mK)$)
L	=	impingement hole length (m)
\dot{m}	=	mass flow rate (kg/s)
Nu	=	Nusselt number
n	=	number of holes
Pr	=	Prandtl number
Re	=	Reynolds number
T	=	temperature ($^{\circ}C$)
t	=	time (s)
U	=	velocity (m/s)
V	=	volume (m^3)
x, y, z	=	coordinate system
X	=	axial jet-to-jet spacing
Y	=	channel width
Z	=	separation distance (channel height)

Greek symbols

θ	=	temperature ratio = $(T-T_o)/(T_g-T_o)$
μ	=	dynamic viscosity [$kg/(ms)$]
ν	=	kinematic viscosity (m^2/s)
ρ	=	density (kg/m^3)
τ_c	=	time constant (sec)

Subscripts

avg	=	average
D	=	hole diameter
d	=	junction diameter
g	=	gas
o	=	initial
i	=	time step index
j	=	jet
p	=	plenum
ss	=	steady state
TC	=	thermocouple
w	=	wall
jct	=	thermocouple junction

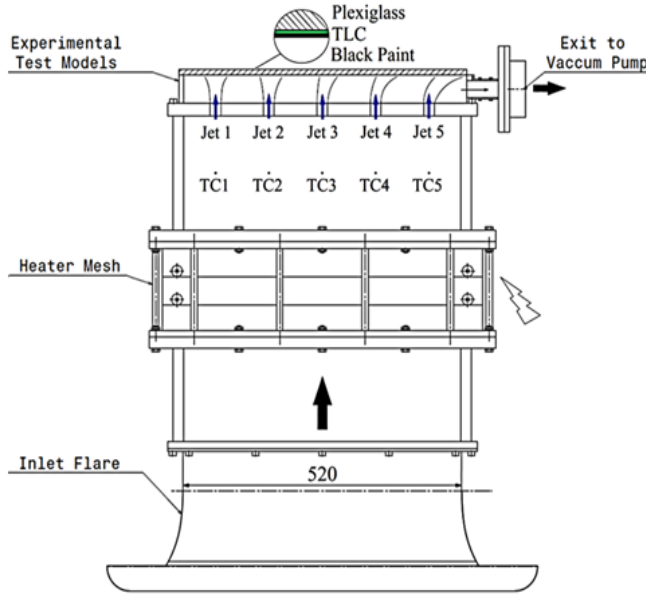


Table 1 Thermocouple characteristics

Thermocouple Number	Thermocouple Type	Wire diameter [mm]
TC1	K	0.08
TC2	K	0.13
TC3	K	0.25
TC4	K	0.51
TC5	K	0.81

Fig. 1 Test facility and thermocouple characteristics

EXPERIMENTAL SETUP

The general arrangement comprises an open circuit wind tunnel operated in suction mode. An overall schematic representation of the wind tunnel is shown in Fig. 1. The low speed wind tunnel consists of the inlet flare, based on McKenzie (1966) [16], a straight section of square ducting that contains the heater grid configuration, the working section which includes the large-scale test models sprayed with liquid crystals, the exhaust pipe and the driving pump. The stainless steel mesh used in this study, is of woven construction, where the wire diameter and the aperture are $25\mu\text{m}$ and $40\mu\text{m}$ respectively, resulting in an open area (mesh porosity) of 38%. The heater mesh covers the whole flow path of the plenum upstream of the impingement plate composing an effective heating area of $520 \times 150\text{mm}^2$ relating to one of the largest mesh heaters (Neely *et al.* (1997) [17]). Power to the mesh is supplied through a 30 kW DC -Power supply whose response time needed to reach steady state conditions has been measured less than 80ms and hence is adequate for the creation of the temperature step in the flow.

Experiments were carried out using two different narrow impingement channels. Both of them include a single row of five inline impingement holes drilled on the impingement plate of the passage so that $L/D=1$, while a single exit mode has been chosen in order to investigate the effect of crossflow generated by the spent air of the jets, representing a realistic situation. All the impingement jets are supplied from the same plenum chamber and therefore have the same total pressure. The axial jet-to-jet spacing and the passage width remained constant at $X/D=Y/D=5$ at a low separation distance of $Z/D=1$. The experimental test models have been manufactured by transparent acrylic material so that the observation of the liquid crystals is performed on the back side of the target plate.

The air exits the impingement channel to a plenum chamber (not shown here) and then to a vacuum pump. The flow rate was adjusted by an inlet vane placed at the suction port of the pump while the mass flow rate was controlled via a laminar flow element mounted in a long duct upstream of the vane pump. This configuration provided the flexibility of very fine regulation of the main stream velocity inside the open circuit wind tunnel. The jet average Reynolds number, based on hole diameter, can be calculated from the total massflow divided by the number of jets used as follows:

$$Re_D = \frac{U_j D}{\nu} = \frac{4\dot{m}}{n\pi D\mu} \quad \text{Eq. 1}$$

where, n , is the number of holes, D [m], is the jet diameter and μ [kg/(ms)] is the dynamic viscosity of the air calculated on the liquid crystal temperature. Several Re_D were investigated in the range of 15000 and 55000, representing realistic engine flow conditions. The uncertainty in the determination of massflow rate was always below 5%.

MEASUREMENT TECHNIQUE AND INSTRUMENTATION

The experiments were carried out using the transient liquid crystal technique. In a typical transient heat transfer experiment, the flow temperature is subjected to a sudden temperature step and the optical response of the liquid crystal surface coating is monitored using a digital video camera at the back of the target plate. Liquid crystals are sprayed on the surface of the target

plate using an air brush while black paint is applied above them in order to create a black background providing brilliant colors. If the thermal conductivity of the model is sufficiently low, the wall temperature response is limited to a thin layer near the wall surface while the lateral conduction is assumed relatively small and hence negligible (Kingsley-Rowe *et al.* (2005) [18]). Therefore, the heat conduction into the model can be assumed to be one-dimensional and a semi-infinite medium approach is used. Numerical and analytical techniques can be used to solve the 1-D transient conduction equation. The relation between the wall surface (liquid crystal) temperature, T_w , and the heat transfer coefficient, h , for the semi-infinite case is then described in many heat transfer textbooks by (Incropera *et al.* (2006) [19]):

$$\Theta_w = \frac{T_w - T_o}{T_g - T_o} = 1 - e^{\beta^2} \operatorname{erfc}(\beta); \quad \beta = h \sqrt{\left(\frac{t}{\rho_w c_w k_w}\right)} \quad \text{Eq. 2}$$

However, in a typical impingement experiment the ratio between the total flow areas of the jets to the flow path of the plenum feeding the jets is far below unity resulting in very low plenum velocities, usually less than 1m/s. According to Ireland and Jones (2000) [4] this is the limit where flow switching needs to be performed for higher heater mesh efficiencies while a step change in the power settings does not cause a step change in the flow. In this case, Duhamel's superposition theorem can be applied to Eq. 1, similar to Poser and von Wolfersdorf (2011) [5], approximating the real temperature evolution by a number of ideal temperature steps as follows:

$$T_w - T_o = \sum_{i=1}^N [1 - e^{\beta^2} \operatorname{erfc}(\beta)] \times \Delta T_{(i,i-1)} \quad \text{Eq. 3}$$

The 1-D transient conduction equation is then solved numerically evaluating the heat transfer coefficient. A narrow bandwidth type of TLCs was used for all experiments (38.5°C-39.8°C). Liquid crystals were calibrated *in-situ* using a surface thermocouple glued on the target plate of the channel. Dark green and light blue colors were considered for the post-processing. The evolution of the liquid crystal color was recorded with a high definition RGB camera (AVT Pike F210C) connected with a frame grabber of 800Mbit/s to the tower of an 8GB-RAM PC. The recorded video data were digitized at a frame rate of 25fps. Uniform and strong illumination throughout the length of the test rig was provided by a pair of two white fluorescent lights (color temperature - 6000K) mounted on both sides of the test rig in order to avoid shadows and reflections.

The hot gas temperature was measured by a set of five K-type thermocouples with exposed junction from OMEGA and equally distributed inside the plenum, as shown in Fig. 1. Each thermocouple had a different wire diameter while the plenum temperature was acquired with a data acquisition system via LabVIEW at a rate of 25Hz in order to minimize the time step effect on Eq.3 (Kwak (2008) [12]). Thermocouple characteristics are indicated in Table 1.

THERMOCOUPLE TIME CONSTANT AND CORRECTION FOR THERMAL INERTIA

Thermocouple response time

The ratio between the total flow areas of the jets to the flow path of the plenum feeding the jets is approximately 0.02 in the case of this study. Subsequently, the velocities in the plenum are in the order of 1m/s or even less and therefore the time response of the thermocouples is sufficient for causing an extra delay missing the capture of the real gas temperature evolution.

Fig. 2(a) indicates the evolution of different thermocouples over a range of various temperature steps at a plenum velocity of 0.5m/s. As expected, the smaller the wire diameter, and hence the connection junction, the quicker is the thermocouple response at a given temperature step. Steady state conditions are reached after approximately 10sec for a very fine thermocouple with a wire diameter of 0.08mm, while the indication temperature of a relatively thick thermocouple (0.81mm) does not perfectly reach the asymptotic value even if the time after the initiation of the heating step is 100s. Additionally, the non-dimensional temperature rise (Θ) is independent of the heating step suggesting a negligible effect of temperature level on the response of the thermocouples. The duration of a transient heat transfer experiment may last between 20s and 80s and therefore a relatively fine thermocouple is required in the plenum so that to provide information about the steady state hot gas temperature which drives the transient experiment.

In such a case, the lumped capacitance method can be used where the real hot gas temperature evolution of the plenum can be extracted from the thermocouple acquisition measurements as follows:

$$-h_{d,jct} A_s [T - T_g(t)] = \rho_{TC} V_{TC} c_{TC} \frac{dT}{dt} \Leftrightarrow T_g(t) = T_{TC,i} + \frac{T_{TC,i+1} - T_{TC,i}}{1 - \exp(-\Delta t / \tau_c)} \quad \text{Eq. 4}$$

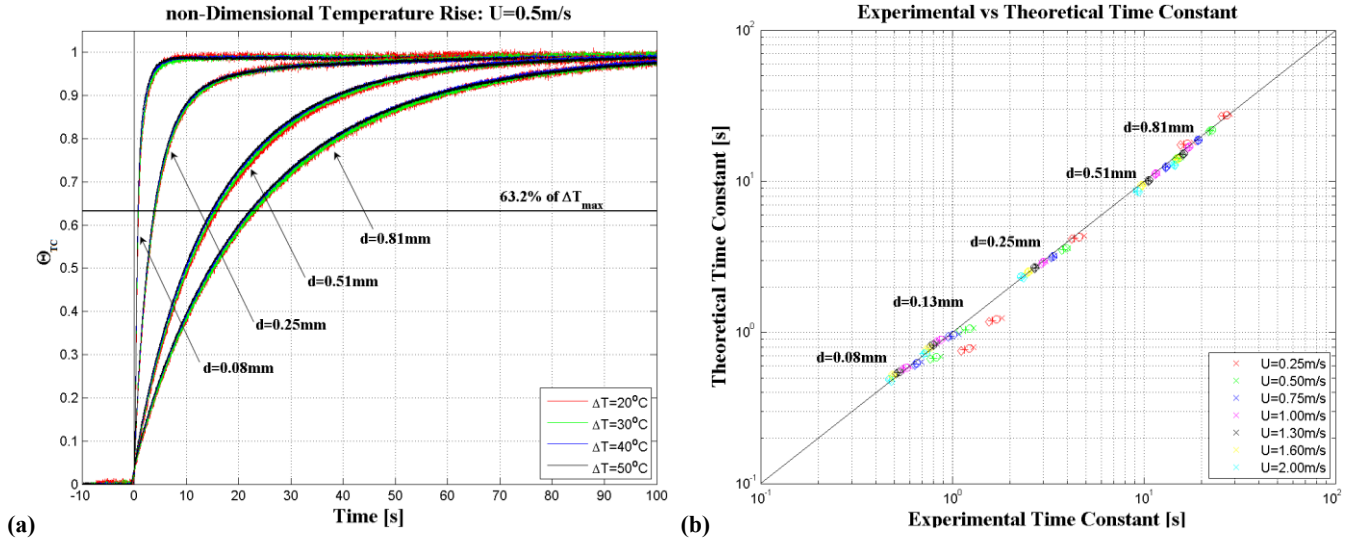


Fig. 2 (a) Temperature steps of various thermocouples. Plenum velocity, 0.5m/s (b) Comparison of $\tau_{c,th}$ and $\tau_{c,exp}$ at various temperature steps and plenum velocities (\square $20^\circ C$, \circ $30^\circ C$, \circ $40^\circ C$, \times $50^\circ C$)

where $\rho_{TC}=8730kg/m^3$ and $c_{TC}=550J/(KgK)$ are the density and the specific heat of the junction material, calculated for a thermocouple wire pair as the average of the thermocouple wire (Chromel-Alumel) properties and $\tau_{c,th}$ is the theoretical time constant of the thermocouple based on the junction diameter (taken equal to approximately 2.5 times the wire diameter):

$$\tau_{c,jct} = \frac{\rho V_s c}{h_{d,jct} A_s} = \frac{\rho d_{jct} c}{6 h_{d,jct}} \quad \text{Eq. 5}$$

Finally, $h_{d,jct}$ is the heat transfer coefficient ($W/m^2 K$) calculated by the well-known Whitaker (1972) [20] correlation:

$$\overline{Nu}_{d,jct} = \frac{h_{jct} d}{k} = 2 + \left(0.4 Re_{d,jct}^{0.5} + 0.06 Re_{d,jct}^{0.66} \right) Pr^{0.4} \left(\frac{\mu}{\mu_s} \right)^{0.25} \quad \text{Eq. 6}$$

Several experiments were carried out evaluating the behavior and the time constant of various thermocouples at different temperature steps and plenum velocities. The theoretical time constant was calculated by Eq. 5 and 6. Physically, this number represents the it time takes for a system's step response to reach 63.2% of its final asymptotic value (Incropera *et al.* (2006) [19]) and therefore the theoretical time constant ($\tau_{c,th}$) was compared with the experimental time constant ($\tau_{c,exp}$) which was assumed to be the time required to reach the 63.2% of the steady state hot gas temperature for a given thermocouple size and temperature step.

Fig. 2(b) shows a comparison of the theoretical thermocouple time constant, calculated from Whitaker's correlation [20] assuming that the thermocouple junction approaches a spherical profile, and the experimental one. Generally, good agreement is observed over the entire range of plenum velocities, wire diameters and different temperature steps. However, at very low plenum velocities ($U_p=0.25$ and $0.5m/s$) and very fine thermocouples ($0.08mm$ and $0.13mm$ wire diameter) a deviation from the $y=x$ line appears. This could be attributed to the very low $Re_{d,jct}$ based on junction diameter, and the inapplicability of Whitaker's equation, which is usually applied for $Re_d > 3.5$. At each wire diameter group in the chart, a reduction of time constant with the plenum velocity is observed, however, the impact of thermocouple size is greater than the airstream velocity in the response of each thermocouple. This is better visible in Fig. 3(a) where the time constant is plotted as a function of plenum velocity for various thermocouples and temperature steps. At a given thermocouple size the time constant is reduced by approximately 50% as the plenum velocity is increased from $0.25m/s$ to $2m/s$. On the other hand, at a given plenum velocity, the time constant can be reduced by a factor of 25 if the wire diameter of the thermocouple is reduced from $0.81mm$ to $0.08mm$. Fig. 3(b) indicates that as the temperature step increases the time constant remains at the same level for all tested thermocouples. This is similar to the results of Farahmand and Kaufman (2006) [21], although a small reduction is observed at small wire diameters.

Calculation of hot gas temperature

Fig. 4 indicates the hot gas temperature, which drives the transient experiment, extracted from Eq.4. For the calculation of the real plenum temperature, the experimental time constant was used thanks to the good agreement with the theoretical one although it has been proven very little difference on the final results. Fig. 4(a) indicates that the extracted plenum temperature is

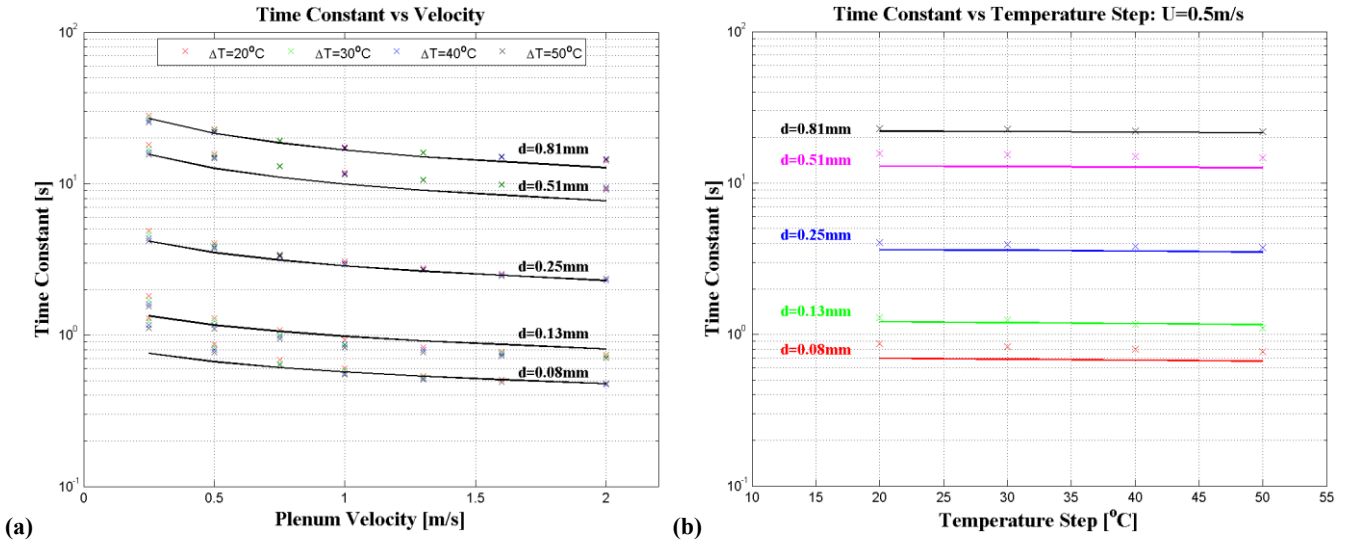


Fig. 3 Time constant as a function of (a) plenum velocity and (b) temperature step (x experimental time constant, – theoretical time constant)

independent on the size of thermocouple which means that the series of the five thermocouples (TC1 to TC5) experience the same plenum temperature evolution. However, a noisy behavior can be observed where the noise fluctuations depend in a very great extent on the thermocouple size. As shown earlier, for a given type of thermocouple, the diameter of the junction is the most important parameter which affects the time constant. Obviously, the smaller the junction diameter (and hence the time constant), the smaller is the denominator of Eq.4 resulting in a more stable extraction of the plenum temperature. On the other hand, plenum velocity has a smaller impact on the denominator of Eq.4 and therefore the level of fluctuations in the extracted temperature is independent on the freestream velocity as shown in Fig. 4(b).

In all the examined cases, an overshooting of the plenum temperature can be observed directly after the initiation of the heating step. This is attributed to the transient response of the DC-Power supply where an overshooting of the supplied power is observed followed by small oscillations which are however within the experimental uncertainties. Fig. 5(a) shows the power supplied in the heater mesh for the case of $Z/D=1$ normalized with the power required to heat a flow of $Re_D=55000$ at $\Delta T=30^\circ C$, approximately $2.4kW$. The duration of power overshoot is relatively small, in the order of $0.05s$, however affects unavoidable the temperature of the heater mesh, the only source of resistance in the circuit, and subsequently a thermal shock is generated inside the plenum approaching the impingement plate. Note also that the temperature step is reduced with increasing Reynolds number so that to achieve a relatively constant liquid crystal first appearance time for all the experiments in the order of $1.5-2s$.

Fig. 5(b) indicates the evolution of the hot gas temperature, $T_g(t)$ during the transient experiment. In this figure the three different approaches are presented: (1) the ideal temperature step, (2) the acquired temperature data of a thermocouple

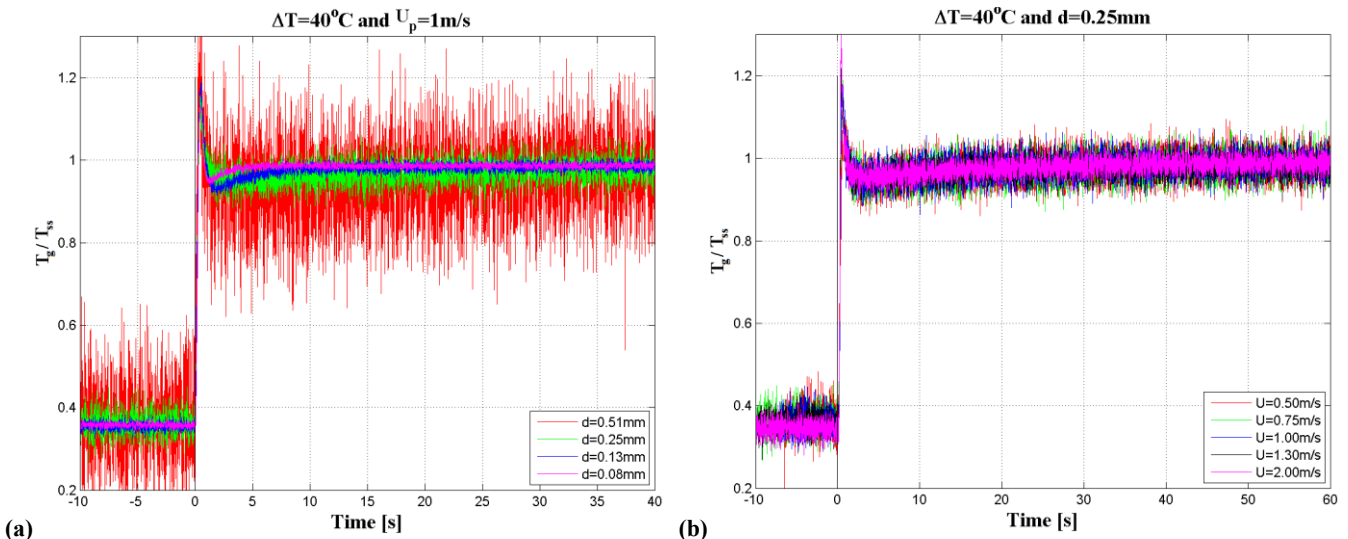


Fig. 4 Unsmoothed hot gas temperature calculated for (a) different thermocouple size and (b) plenum velocities

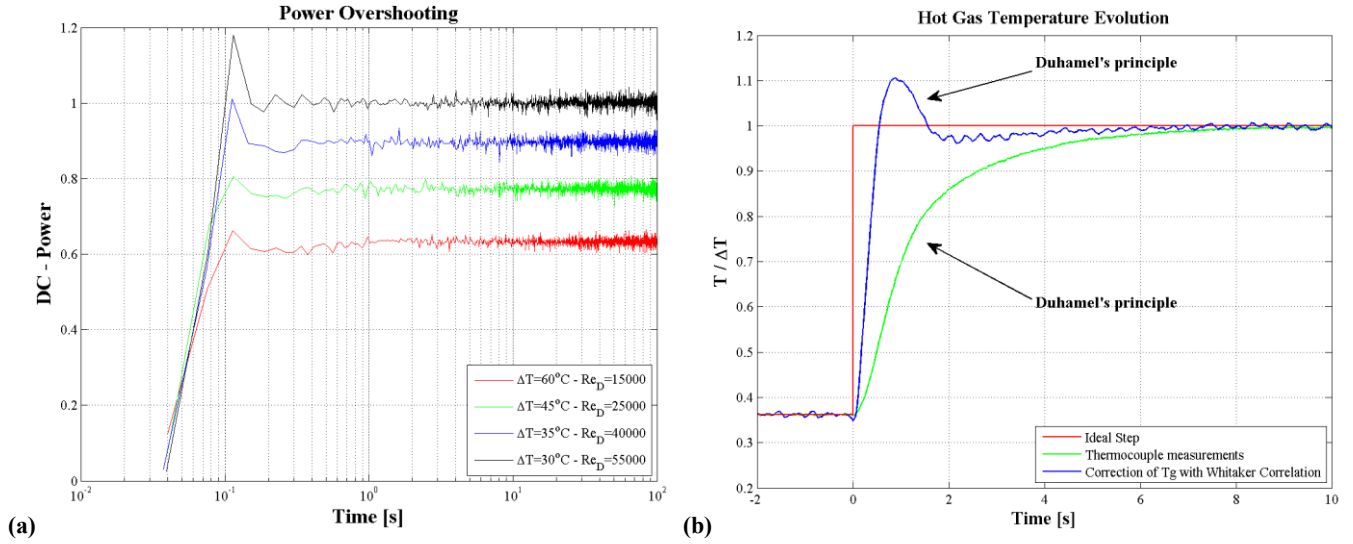


Fig. 5 (a) Power supplied in the heater mesh, $Z/D=1$ (b) Hot gas temperature evolution, $\Delta T=35^\circ\text{C}$

($d=0.13\text{mm}$) placed in the middle of the plenum and (3) the hot gas temperature calculated from Eq.4-6. According to the thermocouple measurements, steady state conditions are reached after approximately 8sec, however, the thermal inertia of the thermocouple junction affects the acquisition of the real gas temperature evolution. The blue line in Fig. 5(b) corresponds to the corrected gas temperature smoothed with the *Savitzky-Golay* smoothing method. As expected, the temperature increase is much sharper and the overshooting of T_g is still observed after the initiation of the heating step due to the overshooting of the achievable power supplied during the adjustment of the desirable electrical energy according to the heater mesh resistance.

EVALUATION OF HEAT TRANSFER COEFFICIENT

Heat transfer surface contours

Fig. 6 indicates full surface heat transfer coefficient distributions on the target plate of the narrow impingement channel at $Re_D=25000$ and 55000 . These data was calculated with three different hot gas temperature evolution cases: (1) Perfect temperature step in the flow (2) Series of step changes (Duhamel's superposition theorem) on the acquired thermocouple measurements (3) Series of step changes on the corrected hot gas temperature considering thermocouple thermal inertia characteristics. The heat transfer coefficient values are normalized with the maximum value appeared on the data in the case of an ideal temperature step, which were approximately $205\text{W}/(\text{m}^2\text{K})$ and $370\text{W}/(\text{m}^2\text{K})$ for a Re_D of 25000 and 55000 respectively.

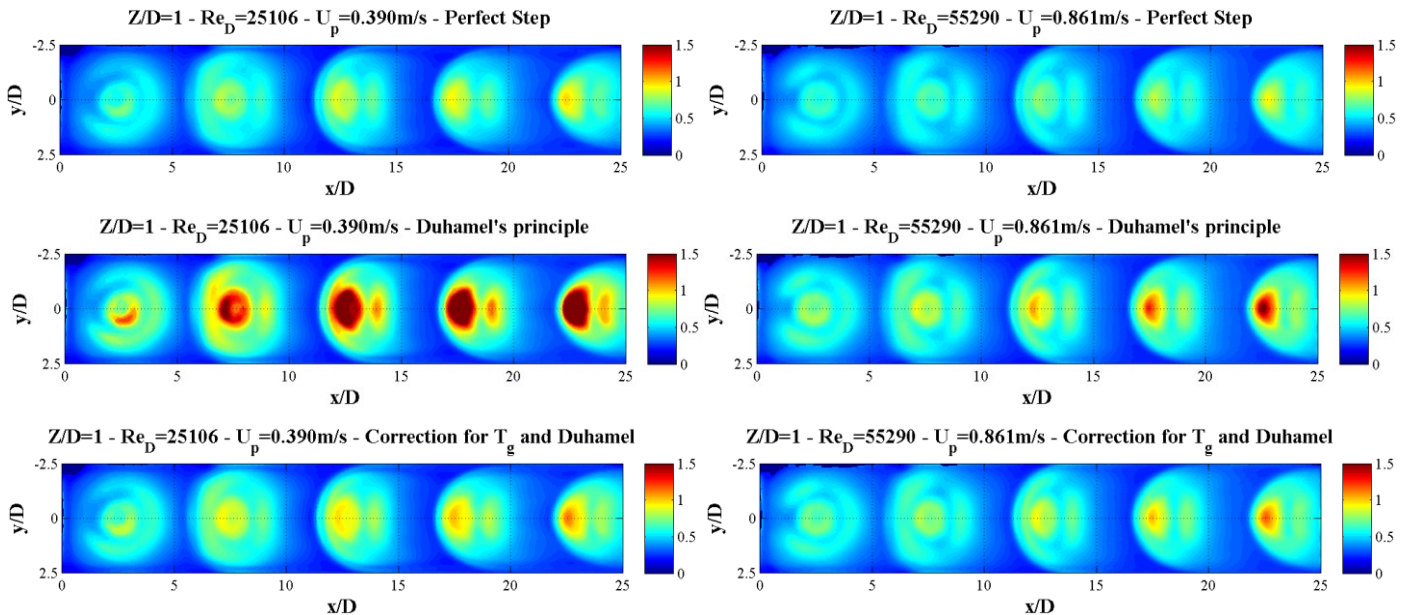


Fig. 6 Heat transfer coefficient surface contours for various hot gas temperatures (a) $Re_D=25000$ (b) $Re_D=55000$

The heat transfer rate distribution is symmetrical along the x –centerline. As the flow accelerates to the exit of the channel the effect of crossflow generated by the spent air of the upstream jet(s) becomes visible. The pattern of the heat transfer coefficient is progressively converted from a circular distribution (Jet 1) to a horseshoe vortex shape distribution (Jet 5). Secondary peaks around the stagnation region of the upstream jets appear similar to single impingement patterns (Baughn and Shimizu (1989) [22]). At Jets 2 and 3 the formation of the horseshoe vortex due to the continuously increased crossflow momentum destroys the circular pattern of the ring. However, the secondary peak is always visible in the wake region downstream of each jet since it is protected somehow from the fluid of the jet. At the last hole (Jet 5) the momentum of the jet is still relatively high compared to the momentum of the crossflow and therefore a similarity with a flow over a cylinder can be observed. Note also that the stagnation point heat transfer coefficient increases for the downstream jets due to the lower static pressure and hence higher local Reynolds numbers.

Although the general flow patterns is similar for the three different cases of hot gas temperature history, the level of heat transfer coefficient is different especially in the stagnation region of the jets where the appearance of liquid crystals is rather quick (1.5-2s). This time of appearance is shorter than the time the thermocouple needs to reach steady state conditions due to its thermal inertia and therefore a relatively lower T_g is considered in the solution of Eq.4. At $Re_D=25000$, where the plenum velocity is $0.39m/s$, the overestimation of the heat transfer coefficient is far above 50% if Duhamel’s superposition principle is applied directly on the thermocouple measurements. On the other hand, a perfect temperature step may result in an underestimation of the heat transfer coefficient since the plenum velocity is low and a step change in the power settings do not cause a step change in the mainstream temperature as well as the temperature overshooting due to the transient response of the DC-Power supply is not considered. For these reasons, Eq.4 5 and 6 was used to calculate the real plenum temperature evolution based on the thermocouple measurements. The level of heat transfer coefficient lies between the aforementioned cases but it is closer to the ideal temperature step assumption. The authors believe that this is not very far from reality since the time needed for DC-Power supply to reach steady state conditions is in the order of $60-100m$ which is still rather quick. At $Re_D=55000$ similar trends are observed, however the plenum velocity is higher ($0.86m/s$) resulting to lower thermocouple time constant. Therefore, the green line in Fig. 5(b) approaches more the ideal step situation and subsequently the differences in the heat transfer level between the three cases are smaller compared to $Re_D=25000$.

Local Nu_D distributions

Fig. 7 indicates the local Nu_D distributions in the centerline of the channel at the same flow conditions from Fig. 6. For both Re_D and a given hot gas temperature evolution approach, at the upstream jets of the channel, a donut shape distribution of Nu_D is observed. However, as the crossflow generated from the spent air of Jets 1 and 2 is developed, the distribution of the heat transfer coefficient is rearranged and slightly shifted in the direction of the flow due to the deflection of the jets. Additionally, the stagnation point heat transfer coefficient increases along the length of the channel due to the decreasing static pressure and hence increasing local Re_D . Regarding the heat transfer level similar trends are observed. An overestimation of the heat transfer coefficient in the stagnation point regions is obtained when Duhamel’s superposition principle is applied directly on the thermocouple data. In this case the level of heat transfer can be more than double compared to the ideal temperature step situation, as for example in the stagnation point of Jet 5 at $Re_D=25000$ which lies at the same level of $Re_D=55000$ and of course

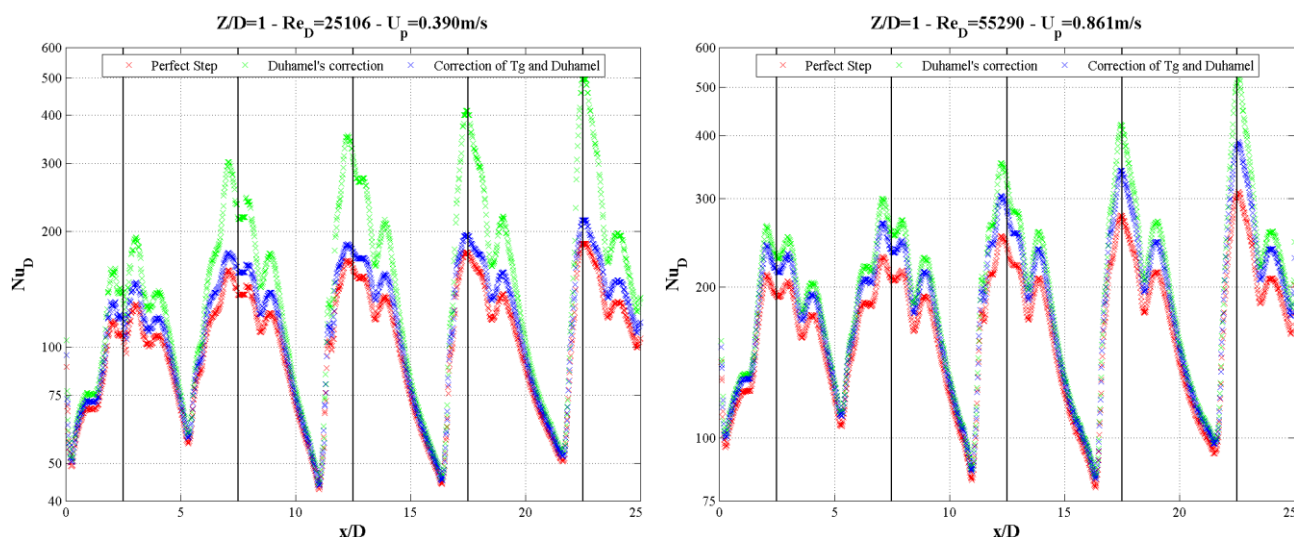


Fig. 7 Local Nu_D distributions for various hot gas temperatures at $Re_D=25000$ and 55000 , $y=0$

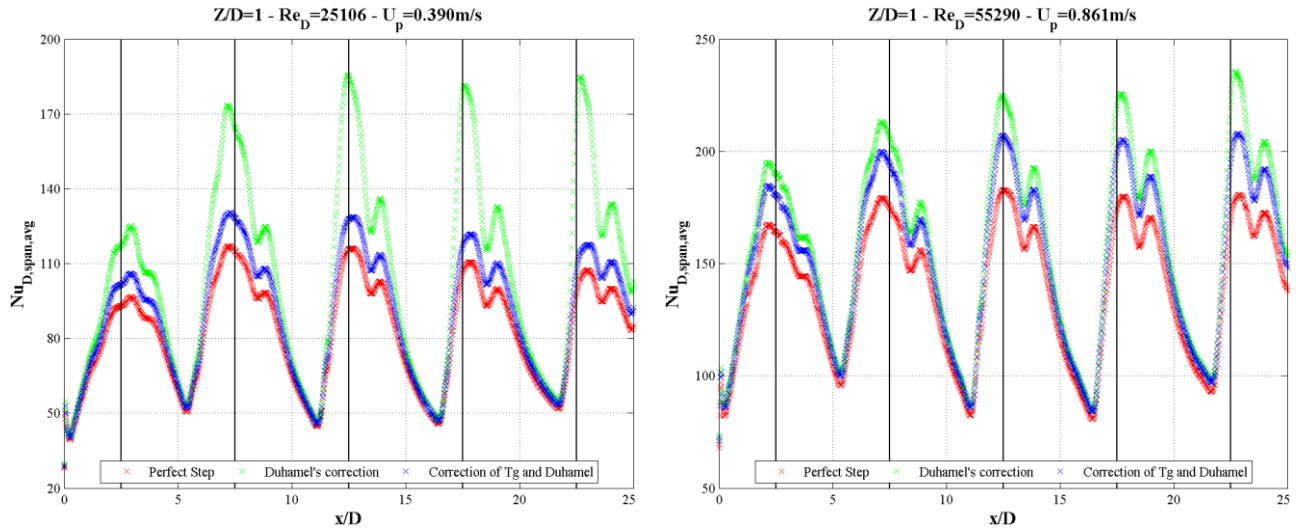


Fig. 8 Spanwise averaged Nu_D distributions for various hot gas temperatures at $Re_D=25000$ and 55000 , $y=0$

represent a non-realistic situation. As discussed earlier, the difference with the ideal temperature step situation is reduced with increasing Re_D (and hence plenum velocity). This is visible at the high Reynolds number of Fig. 7 where the local heat transfer coefficients are apparently closer compared to $Re_D=25000$. However, the Nu_D overestimation compared to the data for the heat transfer rate for the ideal temperature step is 25% for the stagnation region of Jet 1 and approximately 38% for Jet 5. When T_g is corrected prior to Duhamel's superposition principle, the evaluation of heat transfer coefficient results in values in between the above cases. Lower Nusselt numbers agree better as TLC indications appear later in time and therefore the fluid temperature history has a smaller influence on the evaluated data.

Spanwise averaged Nu_D distributions

Fig. 8 indicates the spanwise averaged Nu_D at the target plate of the narrow impingement passage. The increase of stagnation heat transfer from Jet 1 to Jet 5 observed in Fig. 7 is somewhat smoothed out in the spanwise averaged results. The lower stagnation heat transfer of the first jets is compensated by a better lateral coverage of the wall jet due to lower interaction with the crossflow. For the downstream jets, the displacement of the peak heat transfer coefficient values compared to the jet exit positions (black lines) observed in Fig. 7 are also visible in the spanwise averaged results. This was also observed by Bouchez and Goldstein (1975) [23] in a single impingement jet experiment.

Contrary to the local heat transfer distribution of Fig. 7, the Nu_D evaluated with the three different approaches for T_g lie at the same level in the case of spanwise averaged data. This is because the spanwise averaged appearance time of the liquid crystal is larger than the appearance time at the stagnation regions and hence the effect of thermocouple thermal inertia is less intense. In particular, the Nu_D values coincidence at the wall jet regions indicating that the results are nearly independent from the hot gas temperature approach. Maximum difference is in the order of 50% for the stagnation point of Jet 5 and $Re_D=25000$ which is still below the differences observed in the local heat transfer data of Fig. 7. At the higher plenum velocity of $0.86m/s$ the differences are much less and the data seem to agree relatively well also for the stagnation regions of the jets. However, there are still some differences in the order of 10% and 20% from the ideal step for the corrected T_g considering thermocouple thermal inertia and the direct application of Duhamel's superposition principle to the thermocouple measurements.

Area averaged heat transfer data

This section discusses the average heat transfer coefficient obtained on the target plate of the examined test models. In the majority of experiments, a liquid crystal signal could be recorded over 95% or more of the target plate area and therefore, the data are assumed adequate for statistical analysis providing a fairly good representation of the average heat transfer rate. The experimental results of this study have been compared also with various literature data obtained from multi-jet configurations with maximum crossflow orientation and similar geometrical factors (X/D , Y/D and Z/D) and hence open area (Metzger *et al.* (1979) [24], Florschuetz *et al.* (1980) [25], El-Gabry and Kaminski (2005) [26], Xing *et al.* (2010) [27]), Son *et al.* (2001) [28], Ricklick *et al.* (2010) [29]). As expected, Fig. 9 indicates that Nu_D is increased with Reynolds number following a power law of $Nu_D \sim Re^\alpha$. Exponent, α , was estimated to be 0.72 which is a typical value for turbulent boundary layers as expected. More details about the exponent, α , can be found in the study of Terzis *et al.* (2012) [30]. The large scatter in the chart can be attributed to the different geometrical details of the above studies including also nozzle shapes and design, jet turbulence, region of averaging area, mass flow rate determination or even differences of the applied measurement techniques. Nevertheless, good agreement

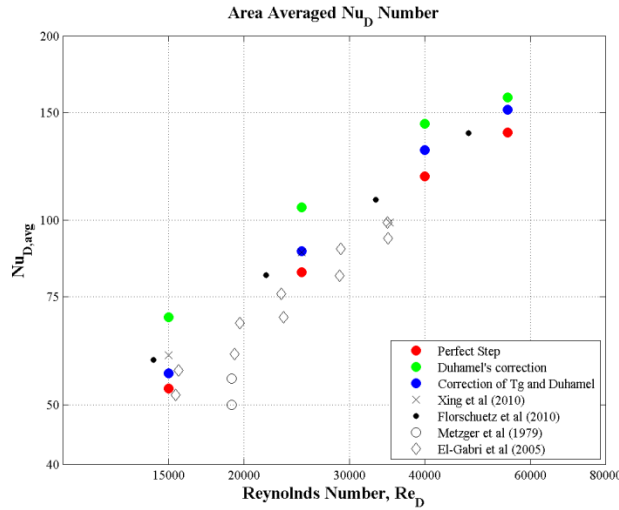


Fig. 9 Area averaged Nusselt number on the target plate

with previous researchers can be observed indicating that the cooling performance of narrow impingement channels in terms of average heat transfer rate on the target plate is comparable with multi-array configurations.

Regarding the optimum hot gas temperature evolution, direct application of Duhamel's principle on the thermocouple measurements without any correction overestimates the heat transfer coefficient as expected; however, the differences in this chart are relatively small compared to the local and spanwise averaged data of Fig. 7 and Fig. 8, due to the fact that the target plate includes also the wall jets regions apart from the stagnation zones where the final results are relatively independent from the hot gas temperature approach, as shown also by the surface contours of Fig. 6. Correction of T_g prior to Duhamel's principle as well as an ideal temperature step are closer to the literature data indicating possibly a more realistic approach to the distribution of the heat transfer coefficient in the stagnation regions and hence have a better approach in the calculation of the average heat transfer rate. In particular, the corrected hot gas temperature data seem to agree relatively well with the results of Florschuetz *et al.* (1980) [21] for $Z/D=1$ over the entire range of Reynolds number.

UNCERTAINTY ANALYSIS

The estimation of the uncertainties associated with the heat transfer results of the current investigation is based on the method of small perturbations, outlined by Moffat (1998) [31], which has been applied in transient heat transfer experiments by Terzis *et al.* (2012) [30] and Chambers *et al.* (2010) [32]. For the calculation of heat transfer coefficient the temperature in the plenum was measured at a sampling rate of 25Hz in order to minimize the effect of time step level in Eq.3, as discussed by Kwak (2008) [12]. The flow temperature measurements indicate a slight increased uncertainty level of thermocouples for the heated flow, which is in agreement with the data of Schueren *et al.* (2011) [33]. The time required for the liquid crystals to reach their calibrated temperature level was evaluated from the recorded video with a frame rate of 25Hz . An extra error, that for the determination of the initiation of the heating step and hence the transient test was estimated in the order of 0.02s while the uncertainty in the thermal properties of Perspex $(\rho_w c_w k_w)^{1/2}$ has been assumed to be 5% according to Ireland (1987) [34]. The effect of each type of measurement error on the heat transfer coefficient is considered alone while the error analysis is performed by applying small perturbations in the test case of $Z/D=1$ and $Re_D=40000$. Table 2 indicates typical values and the uncertainty levels for the heat transfer results and their effect when propagated, in the calculation of the average heat transfer coefficient (typical value $166\text{W}/\text{m}^2\text{K}$). The maximum error can be estimated in the order of 12.6% which is a fairly good value for a transient heat transfer experiment.

Table 2 Experimental uncertainties for the heat transfer results

Parameters	Units	Values	Error	Error in HTC [%]
T_i	[$^{\circ}\text{C}$]	22.9	± 0.12	0.99
T_g	[$^{\circ}\text{C}$]	68.6	± 0.25	1.51
T_w	[$^{\circ}\text{C}$]	39.3	± 0.2	3.18
$\sqrt{\rho c k}$	[$\text{W}\sqrt{\text{s}}/(\text{m}^2\text{K})$]	569	± 29	5.35
t	[sec]	8.84	± 0.1	1.61
HTC_{avg}	[$\text{W}/(\text{m}^2\text{K})$]	166	max error	~ 12.6

SUMMARY AND CONCLUSIONS

In this study, the distribution of the heat transfer coefficients on the target plate of a narrow impingement passage was experimentally measured using the transient liquid crystal technique. The results were evaluated using three different approaches for the hot gas temperature evolution which drives the transient experiment: (1) Perfect temperature step, (2) Duhamel's superposition theorem in the acquired temperature data and (3) Correction of hot gas temperature for thermocouple thermal inertia prior to superposition principle. For the correction of T_g the time constant of thermocouples, which was experimentally measured using various wire diameters and flow conditions, was considered. An uncertainty analysis showed a fairly good repeatability of the measurement technique. The findings of this investigation can be summarized as follows:

1. Thermocouple time constant decreases with reducing the wire diameter and increasing the freestream (plenum) velocity. A negligible effect of the temperature level was observed on the response of thermocouples.
2. Direct application of Duhamel's superposition principle overestimates the local heat transfer coefficients. The faster the appearance time the bigger is the overestimation in the final results which can be more than double, as for example in the local distribution of the stagnation regions of the jets and low Reynolds numbers.
3. Direct application of Duhamel's superposition principle overestimates the area averaged heat transfer coefficient values. The difference from the ideal temperature is 30% and 13% for a $Re_D=15000$ and 55000 respectively. The higher the Re_D the smaller difference between the two assumptions since the plenum velocity is higher and therefore the thermocouple time constant as well.
4. The effect of thermocouple thermal inertia is less intense as the results are averaged in spanwise direction or in the whole target plate area.
5. Lower Nusselt numbers agree better as TLC indications appear later in time and therefore the fluid temperature history has a smaller influence on the evaluated data.

In transient liquid crystal experiments where the thermocouples measuring the driving fluid temperature are located in a low velocity region, it is therefore recommended to correct T_g with the thermocouple thermal inertia prior to Duhamel's superposition principle. This is the case in an impingement configuration where the jets are fed from a common plenum.

ACKNOWLEDGMENTS

This study was performed in the framework of KW2020 (KraftWerke 2020) project funded by the Swiss Federal Office of Energy (SFOE/BFE, Bern, Switzerland) and Alstom (Baden, Switzerland). All the pieces of this test facility have been manufactured in-house in Atelier de l'Institut de génie Mécanique (ATME) of EPFL.

The authors are grateful to Theodoros Kyriakidis (EPFL, Switzerland) and Serafeim Perdakis (EPFL, Switzerland) for their valuable support during the setup of electronic equipment. Special thanks to Prof. Anesits I. Kalfas (Aristotle University, Greece) for the discussions during the construction of the test facility.

REFERENCES

- Weigand B. and Spring S. (2011) "Multiple Jet Impingement - A Review" *Heat Transfer Research*, Vol. **42**(2), pp. 101-142.
- Baughn J. W. (1995) "Liquid Crystal Methods for Studying Turbulent Heat Transfer" *International Journal of Heat and Fluid Flow*, Vol. **16**, pp. 365-375.
- Ireland P. T., Neely, A.J., Gillespie, D.H.R., Robertson, A.J. (1999) "Turbulent Heat Transfer Measurements Using Liquid Crystals" *International Journal of Heat and Fluid Flow*, Vol. **20**, pp. 355-367.
- Ireland P. T. and Jones T. V. (2000) "Liquid Crystal Measurements of Heat Transfer and Surface Shear Stress" *Measurement Science and Technology*, Vol. **11**, pp. 969-986.
- Poser R. and von Wolfersdorf J. (2011) "Liquid Crystal Thermography for Transient Heat Transfer Measurements in Complex Internal Cooling Systems" *Heat Transfer Research*, Vol. **42**(2), pp. 181-197.
- Van Treuren K. W., Wang Z., Ireland P. T. and Jones T. V. (1994) "Detailed Measurements of Local Heat Transfer Coefficient and Adiabatic Wall Temperature Beneath an Array of Impinging Jets" *Journal of Turbomachinery, ASME*, Vol. **116**(3), pp. 336-374.
- Huang L. and El-Genk M. S. (1994) "Heat Transfer of an Impinging Jet on a Flat Surface" *International Journal of Heat and Mass Transfer*, Vol. **37**(13), pp. 1915-1923.
- Falcoz C., Weigand B. and Ott P. (2006) "Experimental Investigations on Showerhead Cooling on a Blunt Body" *International Journal of Heat and Mass Transfer*, Vol. **49**, pp. 1287-1298.
- Wagner G., Schneider E., von Wolfersdorf J., Ott P., et al. (2007) "Method for Analysis of Showerhead Film Cooling Experiments on Highly Curved Surfaces" *Experimental Thermal and Fluid Science*, Vol. **31**, pp. 381-389.
- Gillespie D. R. H., Wang Z. and Ireland P. T. (1995). Heating Element. PCT/G96/2017. Application, B. P.
- Espósito E. I., Ekkad S. V., Kim Y. and Dutta P. (2009) "Novel Jet Impingement Cooling Geometry for Combustor Liner Backside Cooling" *Journal of Thermal Science and Engineering Applications*, Vol. **1**(2), pp. 021001-021008.
- Kwak J. S. (2008) "Comparison of Analytical and Superposition Solutions of the Transient Liquid Crystal Technique" *Journal of Thermophysics and Heat Transfer*, Vol. **22**(290-295).
- Wormser A. F. (1960) "Experimental Determination of Thermocouple Time Constants with Use of a Variable Turbulence, Variable Density Wind Tunnel, and the Analytic Evaluation of Conduction, Radiation, and Other Secondary Effects" *SAE Trans., April 5-8, 1960*, Vol.
- Murdock J. W., Foltz C. J. and Gregory C. (1963) "A Practical Method of Determining Response Time of Thermometers in Liquid Baths" *Journal of Engineering for Power, ASME*, Vol., pp. 27-32.

- Farahmand K. and Kaufman J. W. (2001) "Experimental Measurement of Fine Thermocouple Response Time in Air" *Experimental Heat Transfer*, Vol. **14**, pp. 104-118.
- McKenzie A. B. (1966). An Investigation of Flare Dimensions for Standart and Annular Air Meters. Report, C. D. Derby, UK, Rolls-Royce Plc.
- Neely A. J., Ireland P. T. and Harper L. R. (1997) "Extended Surface Convective Cooling of Engine Components Using the Transient Liquid Crystal Technique" *Journal of Power and Energy A*, Vol. **211**, pp. 273-287.
- Kingsley-Rowe J. R., Lock G. D. and Owen J. M. (2005) "Transient Heat Transfer Measurements Using Thermochromic Liquid Crystals: Lateral-Conduction Error" *International Journal of Heat and Fluid Flow*, Vol. **26**(2), pp. 256-263.
- Incropera F. P., Dewitt D. P., Bergman T. L. and Lavine A. S. (2006). Fundamentals of Heat and Mass Transfer. 6th Edition, John Wiley & Sons.
- Whitaker S. (1972) "Forced convection heat transfer correlations for flow in pipes, past flat plates, single cylinders, single spheres, and for flow in packed beds and tube bundles" *AIChE Journal*, Vol. **18**(2), pp. 361-371.
- Farahmand K. and Kaufman J. W. (2006) "Measurement of Time Constant of Wet-Bulb Thermocouple in Air" *Experimental Heat Transfer*, Vol. **19**, pp. 165-180.
- Baughn J. W. and Shimizu S. (1989) "Heat Transfer Measurements From a Surface With Uniform Heat Flux and an Impinging Jet" *Journal of Heat Transfer, ASME*, Vol. **111**, pp. 1096-1098.
- Bouchez J.-P. and Goldstein J. (1975) "Impingement Cooling From a Circular Jet in a Crossflow" *International Journal of Heat and Fluid Flow*, Vol. **18**, pp. 719-730.
- Metzger D. E., Florschuetz L. W., Takeuchi D. I., Behee R. D., et al. (1979) "Heat Transfer Characteristics For Inline and Staggered Arrays of Circular Jets With Crossflow of Spent Air" *Journal of Heat Transfer, ASME*, Vol. **101**, pp. 526-531.
- Florschuetz L. W., Berry R. A. and Metzger D. E. (1980) "Periodic Streamwise Variations of Heat Transfer Coefficients For Inline and Staggered Arrays of Circular Jets With Crossflow of Spent Air" *Journal of Heat Transfer, ASME*, Vol. **102**(1), pp. 132-137.
- El-Gabry L. A. and Kaminski D. A. (2005) "Experimental Investigation of Local Heat Transfer Distribution on Smooth and Roughened Surfaces Under an Array of Angled Jets" *Journal of Turbomachinery, ASME*, Vol. **127**(3), pp. 532-544.
- Xing Y., Spring S. and Weigand B. (2010) "Experimental and Numerical Investigation of Heat Transfer Characteristics of Inline and Staggered Arrays of Impinging Jets" *Journal of Heat Transfer, ASME*, Vol. **132**, pp. 092201-092211.
- Son C. M., Gillespie D. R. H., Ireland P. T. and Dailey G. M. (2001) "Heat Transfer and Flow Characteristics of an Engine Representative Impingement Cooling System" *Journal of Turbomachinery*, Vol. **123**, pp. 154-160.
- Ricklick M., Kapat J. S. and Heidmann J. (2010) "Sidewall Effects on Heat Transfer Coefficient" *Journal of Thermophysics and Heat Transfer*, Vol. **24**(1), pp. 123-132.
- Terzis A., Wagner G. and Ott P. (2012). Hole Staggering Effect on the Cooling Performance of Narrow Impingement Channels. ASME, TurboExpo 2012, 11-15 June 2012, Copenhagen.
- Moffat R. J. (1998) "Describing the Uncertainties in Experimental Results" *Experimental Thermal and Fluid Science*, Vol. **1**(1), pp. 3-17.
- Chambers C. A., Gillespie D. R. H., Ireland P. T. and Kingston R. (2010) "Enhancement of Impingement Cooling in a High Crossflow Channel Using Shaped Impingement Cooling Holes" *Journal of Turbomachinery, ASME*, Vol. **132**, pp. 021-021 - 021-028.
- Schueren S., Hoeffler F., von Wolfersdorf J. and Naik S. (2011). Heat Transfer in an Oblique Jet Impingement Configuration With Varying Jet Geometries. ASME TurboExpo - GT2011-45169.
- Ireland P. T. (1987). Internal Cooling of Turbine Blades. D. Phil. Oxford University, United Kingdom.